

Quantification of Contact Resistance of Metal Foam Heat Exchangers for Improved, Air-cooled Condensers in Geothermal Power Application

A. Chumpia¹ and K. Hooman¹

¹Queensland Geothermal Energy Centre of Excellence
School of Mechanical and Mining Engineering
University of Queensland, Brisbane, Queensland 4072, Australia

Abstract

Two types of aluminum foam-wrapped cylindrical heat exchanger, with foam layer thickness of 5mm, are being tested for heat transfer performance and pressure drop characteristics. The first heat exchanger, HX1, has the core tube made of S316 stainless steel with the tube external and internal diameters measure 32.0mm and 28.3mm, respectively. The foam layer of HX1 is bonded to its core tube using highly conductive thermal glue. The second heat exchanger, HX2, has the core tube made of AA6061, the same material as the foam layer covering it, and the two parts are bonded together by a brazing technique. The core tube of HX2 has nearly identical dimension to that of HX1 with a small variation in its thickness. The tests are carried out on each heat exchanger, installed horizontally in a cross-flow arrangement inside a wind tunnel, one at a time with air velocity varying between 1.5 to 5 m/s. Heat transfer from 75°C hot liquid, circulating through the core tube, to external air is evaluated using the concept of total thermal resistance where the effects of tube material and the two bonding methods are quantified as a series of smaller resistant components. The results show that, within the range of designated air velocity, thermal contact resistance (TCR) of HX1 is 0.015 ± 0.001 K/W larger than that of HX2; essentially constant with the air flow rate. This TCR however contributes between 10% to 19% of HX1 total thermal resistance from lowest to highest air velocity, respectively. On the other hand, pressure drop results show very close figures between HX1 and HX2. They are steadily increased from 2.0 Pa at lowest air velocity to 19 Pa at highest velocity.

Introduction

Metal foams are highly porous materials consisting of mostly inter-connected and randomly distributed voids called 'cells'. Typically, a cell approximate shape and form is a near-spherical polyhedron having 14 faces. Each cell face forms an open passage called 'pore' to adjacent surrounding cells in all directions. The porous structure as described therefore makes metal foam permeable, and provides very well-mixed patterns, to fluid flows in macroscopic scale. In addition, the solid backbone micro-features maintaining the existence of all cells and pores – termed 'struts' (or 'ligaments', or 'fibres') and nodes (where struts join) – have a combined effect resulting in a very high interfacial surface area between the void and its solid backbone. T'Joen, et al. [13] reported approximate figures for this area to be in a range of $500 \text{ m}^2/\text{m}^3$ to $10,000 \text{ m}^2/\text{m}^3$.

Due to their other unique properties of high strength, high absorption to impact, low weight, excellent noise attenuation, etc., metal foams offer new possibilities in emerging industries where these combined properties are sought. Nevertheless, one distinct application which can take a maximum advantage of all metal foam features and properties mentioned above is that involving high efficiency heat exchange. Three niche technological areas that fit within this broad application are; thermal processes demanding high rate of simultaneous

chemical reactions, fast rate heat removal from high power electronic components, and highly efficient condensers for heat rejection in power cycles operating at low temperature differentials. It therefore comes to no surprise that a larger percentage of open literature on metal foam studies in the past decade has been centred around high performance heat exchangers of some forms [1, 7, 9, 10, 11]. It is also notable that a large number of them either concern fundamental investigations of the materials themselves or practical applications dealing with relatively small metal foam volume. Compact heat sinks for high density electronic circuits are obvious examples. Regardless of detailed designs, however, metal foam used in heat exchangers is usually bonded to a solid substrate which may be a flat metal sheet for a block design or a tube wall for tubular design. Depending on individual thermal systems, the direction of heat flow can be either from foam mass to solid substrate or the opposite; but in both cases heat must flow across the interface between the two. This fact imposes an extra component, the bonding resistance or thermal contact resistance (TCR), in the lump of overall heat transfer resistance of foam-modified surfaces. In their study, T'Joen, et al. [13] found that a 0.3mm thick thermal glue bonding aluminum foam to the outer surface of 12mm aluminum tubes to have a significant impact on heat transfer performance, contributing to a minimum of 6% and up to 55% of the overall resistance to heat flow. Fiedler, et al. [5], studying 6 samples of copper foam, showed that the TCR between solid substrate and cellular metal cannot be predicted reliably using the thickness extrapolation method. Total thermal resistance of the copper foam samples was determined by conducting the measurements inside a specially designed vacuum chamber to eliminate the effect of convective heat transfer. Their study concluded by presenting a linear correlation of TCR flux to foam-substrate contact area.

The objective of this paper is to present and compare thermo-hydraulic performance of two designs of tubular aluminum foam heat exchanger. Focus is given to assessing the effect of different bonding methods used for the two heat exchanger specimens. This work forms a small part of a project aimed at identifying best practices in assembling heat exchangers of this design, and further evaluating their performance in bundle configurations, taking economic into consideration. The target application of heat exchangers studied in this project is an air-cooled condenser in a typical low temperature turbine cycle such as that found in geothermal power plants.

Specimen Description

Both specimens used in this performance test are ready made commercial products. Heat exchanger 1, abbreviated 'HX1', was manufactured by wrapping a rectangular section of aluminum foam around a 316 stainless steel tube. The foam has a dimension of $100.5 \times 455.0 \times 5.0 \text{ mm}^3$ with its other characteristics as shown in table 1. The stainless steel tube has external diameter, D_o , of 32.0mm, internal diameter, D_i , of 28.3mm, and a total length of 580.0mm.

Foam type	PPI	ϕ	$\sigma_0 [m^{-1}]$	% Al
HX1	20	0.937	720	99.5
HX2	20	0.901	870	98.6

Table 1: Properties of aluminum foam used in HX1 and HX2.

The foam section was attached to the tube surface by first applying a thin layer, 0.3 – 0.6 mm, of conductive epoxy glue around the tube. The foam was then gradually rolled into a cylinder with the curvature as close as possible to the outer contour of the tube, hard pressed onto the tube surface and into the glue layer, then tied around with a thin wire. Finally, the whole assembly was cured inside an oven set at 150°C for about an hour.

In table 1, the PPI is a non-dimensional number specifying how many pore-size equivalent circle can be placed side-by-side on a linear inch. The higher the PPI number, the less ‘open’ the foam is. Porosity (ϕ), also a non-dimensional number, is a ratio of void space to the total foam volume. As the void space is not easily measured, in practice porosity is determined indirectly but quite accurately by weighing the sample. Together with the density of its base material and the volume of the original sample, void volume and solid volume can be determined. The third column in the table lists a property called surface-to-volume ratio (σ_0, m^{-1}). This property offers a convenient means for calculating the foam interfacial surface area, ISA, when its volume is known. HX1 properties listed in table 1 were published by De Jaeger, et al. [3] where the ISA was determined using a micro-computed tomography (μ CT) scanning technique. For HX2, the PPI and porosity measurements were published by its manufacturer while σ_0 is the best match value adopted from [3] based on its porosity.

HX2 was assembled using high temperature brazing to bond the foam mass, made of the 6061 aluminum alloy, to the outer surface of the core tube made of the same material. All foam dimensions of HX1 apply to HX2. HX2 was supplied by a different manufacturer and the detailed process of brazing was not disclosed. However, visual inspection of the specimen reveals a meticulous surface finish, probably by a specialized lathe. As a result, HX2 has a totally uniform thickness of the foam layer (5mm) but physical distortion of strut ends on the surface can still be observed.

Experimental Set-up and Procedure

The test facility is an open-circuit wind tunnel shown in figure 1. The air is drawn into the tunnel from the right-hand side through fine screen filters and honeycomb separator, passing through the constriction plenum (4) into the test section (3). In the test section, the air mass which flows over the hot surface of the heat exchanger (HX1 or HX2) takes up heat, flows into the stabilizing chamber (1) and exits through the elbow bend (not shown) which diverts the exhaust air out of the system via the ceiling. Just before the elbow, the suction blower is installed in-line and the driving shaft extends out to the prime mover which is a large 17kW electrical motor. The constriction section has one pressure ring at its inlet and another at the exit where it joins the test section. The pressure differentials of the two rings are input to a transducer which generates a signal to drive the control unit for the blower motor. The air velocity can therefore be controlled using a PID, closed loop system. Before the test, the air velocity is verified by the Particle Image Velocimetry (PIV) measurement (6) under the empty chamber condition.

The test section has its cross-sectional areas measured 454mm \times 454mm at the inlet and 462mm \times 462mm at the exit. It is 1220mm long and divided into three compartments horizon-

tally. The middle compartment has the cross-sectional area of 454mm W \times 210mm H at its inlet. During the experiments, the heat exchanger specimen is installed in the centre line of the middle section. A pair of pitot tube are installed either side of, and at the same level to, the specimen to measure the pressure drop. The upstream pitot tube, the specimen, and the downstream pitot tube, are located 193mm, 455mm, and 810mm, respectively from the test section inlet. The pressure drop is recorded by a high accuracy pressure differential transducer with a resolution of ± 0.01 pa at 200 Pa full scale. A pair of PT-100 RTD probes are installed in the bottom compartment near the test section inlet to measure the air inlet temperature. Exit temperature was measured by an XY traversing system (2) where four PT-100 probes are mounted and can scan the designated exit area of the three compartment at the grid size of 10mm \times 10mm.

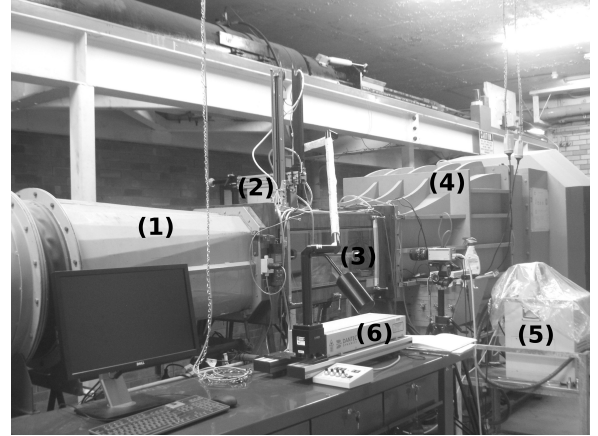


Figure 1: The wind tunnel facility being used in the experiments

On the liquid side, a hot liquid mixture—made of 1 part of a concentrated automotive coolant + 2 parts water by volume—is heated and maintained at 75°C by a heater/cooler unit (5). The hot liquid circulated around a closed circuit through the core tube of the heat exchanger. Inlet and exit liquid temperature as well as its flow rate are measured. Data logging and control of different parts of the system such as air velocity and exit air temperature scanning are co-ordinated by a host computer. Before testing the foam-wrapped specimens, a plain aluminum cylindrical tube, D_o 30mm D_i 26mm is installed for a reference run. The Nusselt numbers according to Hilpert and Zukauskas as described by [8] are verified and found to be agreeable. This ensures the validity of the test rig.

For each specimen under test, The air flow is set and the liquid temperature at heat exchanger inlet is monitored until it is settled within $75 \pm 0.75^\circ\text{C}$, all relevant data are logged every second for 10 mins. The air flow is then increased to the next step at 0.5 m/s increment and when the liquid temperature re-settles, the process is repeated until the maximum velocity of 5.0 m/s is reached.

Data Analysis

Thermal exchange analysis follows theoretical formulation of related parameters in a cross flow. As the hot liquid mixture enters the heat exchanger core and flows to the exit, it loses heat to the cooler airstream flowing past the heat exchanger external surface. This exchange of thermal energy occurs inside the test section and the total heat transfer, \dot{Q} [W], is evaluated from:

$$\dot{Q} = \dot{Q}_{liq} = \dot{m}_{liq} \bar{c}_p \Delta T \quad (1)$$

where \dot{m}_{liq} is the mass flow rate of hot liquid [kg/s], \bar{c}_p is its specific heat capacity at fixed pressure [J/kg.K], and ΔT is the temperature differential of liquid mixture at the inlet and exit of the heat exchanger = $T_{liq,in} - T_{liq,out}$ [K].

The effect of radiation heat transfer between the heat exchangers and their surroundings inside the test section is insignificant and therefore is not included in the calculation. By tracing the heat flow path from the liquid to the air side, the components making up the overall thermal resistance (R_t [K/W]) can be easily identified. Together with its definition, this is written as:

$$\frac{(T_s - T_\infty)}{\dot{Q}} \equiv R_t = R_{hliq} + R_k + R_c + R_{ha} \quad (2)$$

where T_s is surface temperature of the heat exchanger [K], T_∞ is the free stream temperature of the air [K], and \dot{Q} [W] is as calculated by equation 1. The component resistances [K/W] listed on the right-hand side, from the liquid side to the air, are those due to: convective action at the inside wall–liquid interface, R_{hliq} ; conductive action through the tube wall, R_k ; contact bonding of the foam layer to the tube surface, R_c ; and convective action at the foam–air interface, R_{ha} , respectively.

Further:

$$R_t = \frac{1}{h_{liq} A_t} + \frac{\ln \frac{r_o}{r_i}}{2\pi k_t L} + R_c + \frac{1}{h_a A_s \eta_f} \quad (3)$$

here h_{liq} is the convective heat transfer coefficient on the liquid side [W/m².K], and A_t is the tube internal surface area taking part in exchanging heat between hot liquid and the tube wall [m²]. On the conductive term, r_o is the external radius of the core tube not including the foam thickness [m], r_i is its internal radius [m], k_t is thermal conductivity of the core tube material [W/m.K], and L is the length of the core tube section covering with foam and approximately equal to the test section width [m]. R_c is the thermal contact resistance being investigated.

The last term of equation 3 is worth further elaboration as it represents the site where augmentation of heat transfer due to surface modification is promoted. In parallel to those in the first term, h_a is the convective heat transfer coefficient of the foam–air interface [W/m².K] while A_s is the interfacial surface area between the air, including that filling the void, and the foam solid structure. In studying the effect of different bonding methods on TCR between open-cell aluminum foam and its flat metal substrate, De Jaeger, et al. [4] provided a thorough descriptive detail on η_f and the approach they used to quantify it by following the work done earlier by Ghosh [6]. η_f is a dimensionless number known as ‘fin efficiency’. It describes the effect of conductive resistance within solid matrix of the foam where convection mode of heat transfer is dominant.

In this study, it is also assumed that—under steady conditions—the internal surface of the core tube and the bulk liquid mixture flowing inside it are at the same, fixed temperature due to high heat flow rate. In other words, the thermal resistance due to convection heat exchange between the inside surface of the core tube and the high temperature liquid is negligible.

Results and Discussion

The foam materials covering HX1 and HX2 are of similar alloy ($k \sim 220 - 235$ W/m.K), having the same PPI density, and

applied to their respective heat exchanger with the same thickness. Because of this, the last component of equation 3 will be evaluated to nearly the same figure.

Following the argument and assumptions outlined above, comparison of the TCR of HX1 and HX2 by rewriting equation 2, nullifying R_{hliq} in both cases because their values tend to zero, and cancelling out the two R_{ha} because they have nearly identical figure range, produces the end result:

$$(R_c)_{HX1} - (R_c)_{HX2} = (R_t - R_k)_{HX1} - (R_t - R_k)_{HX2} \quad (4)$$

The left-hand expression of equation 4 represents ΔTCR . It is plotted against air velocity as shown in figure 2.

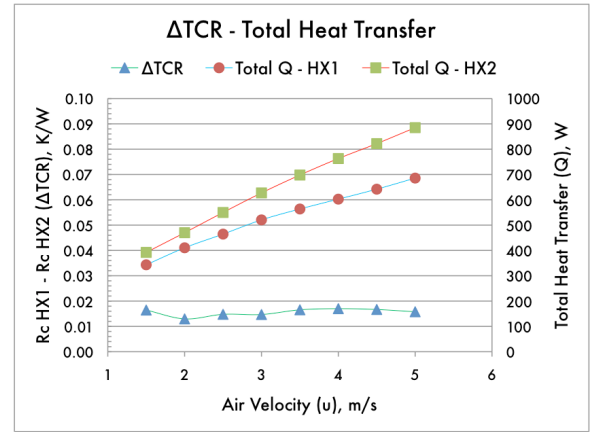


Figure 2: ΔTCR and total heat transfer of HX1 and HX2 and their variations with air velocity.

From figure 2, it is obvious that HX1 is less efficient in rejecting heat at the same range of air velocity. This agrees with the fact that ΔTCR as defined by equation 4 is positive, i.e. it has higher TCR than HX2 does. In open literature, no quantification of TCR for brazed bonding is found [4] because it is generally accepted that brazing method offers negligible TCR ([2, 12] - among others). If this criterion is adopted, it can be concluded that the absolute TCR of the thermal glue used in bonding for HX1, as applied to the test conditions described in this study, is constant at 0.015 ± 0.001 K/W across the range of air flow. However, it can be observed from figure 2 that, at higher air velocity, total heat transfers on HX1 and HX2 continue to diverge. The interpretation here is ΔTCR has more significant effect on the heat transfer performance at lower air velocity. At higher air velocity, other factors such as thermal conductivity and variation in thickness of the core tube likely have stronger effects on the total heat transfer than TCR does. To appreciate TCR effect, if the resulting figure is normalized against the overall thermal resistance for HX1, TCR contributes between 10% to 19% of HX1 total thermal resistance from the lowest to the highest air velocity.

Figure 3 shows the comparison of the pressure drop on each heat exchanger under study. As can be seen, there is no significant difference on hydraulic behavior between HX1 and HX2 when they are subject to similar test conditions. This is to be expected as pressure drop is known to be affected by tangible, macroscopic properties of the specimens. Because HX1 and HX2 have very similar physical dimensions and foam specifications, their pressure drop results are therefore predictively

similar. The thin layer of thermal conductive glue being added on the external surface of HX1 tube core to bond its foam matrix doesn't manifest a different effect to the results.

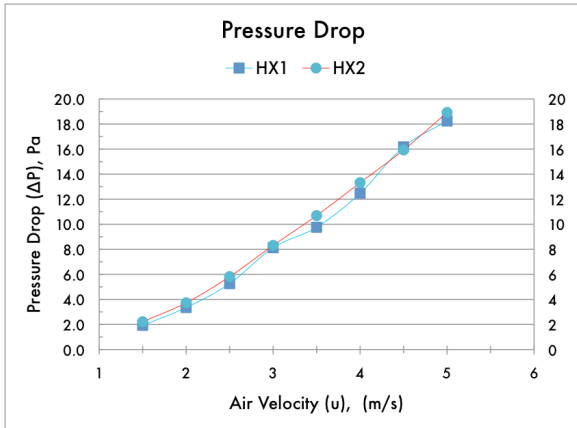


Figure 3: Comparison of pressure drop caused by HX1 and HX2 when tested under air velocity variation.

It has been mentioned earlier that HX2 was manufactured with high standard and the foam layer was machined to a uniform thickness. In contrast, HX1 does not boast this construction quality and contains split edges where the two ends join as the foam section was wrapped around the core cylinder, as shown in figure 4. However, this cosmetic detail doesn't produce a large scale negative effect on HX1 hydraulic performance as compared with HX2, which can be readily confirmed from the two curves shown in figure 3.

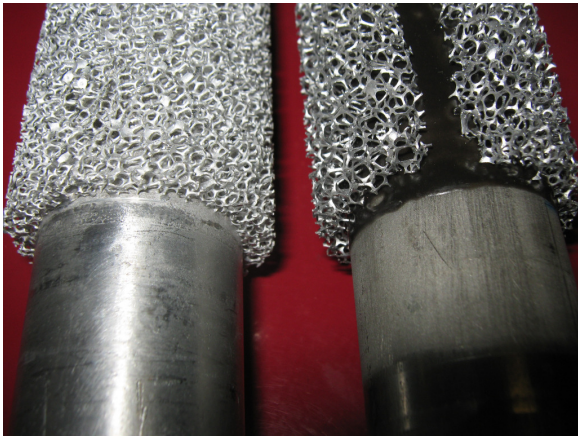


Figure 4: Imperfection of foam layer assembly on HX1 (right) comparing with foam layer on HX2 (left). The thermal glue layer between the foam and tube wall is clearly visible at the split

Conclusions

Open cell metal foams have been studied widely as novel materials for many emerging technologies. Among these, one application of interest which can take maximum advantage of the foam properties is heat exchanger. In this study tubular design of two heat exchangers employing foam to enhance their performance is analyzed for TCR evaluation. Bonding techniques affect thermal performance of the two heat exchangers under

study, but they don't affect the heat exchanger hydraulic behavior. Using the concept analogous to resistance of electrical flow, the resistance to heat flow associated with (non-brazing) bonding the foam mass to the core tube (TCR) is quantified. When the method of bonding is brazing, the resulting TCR is very low, thus allows indirect quantification of TCR as a result of bonding by other methods.

References

- [1] Boomsma, K., Poulikakos, D. and Zwick, F., Metal Foams As Compact High Performance Heat Exchangers, *J. Mech. of Materials*, **35**, 2003, 116–1176.
- [2] Calmidi, V.V. and Mahajan, R.L., Forced Convection in High Porosity Metal Foams, *J. Heat Transfer - Trans. of the ASME*, **122**, 2000, 557–565.
- [3] De Jaeger, P., T'Joel, C., Huisseune, H., Ameel, B. and De Paepe, M., An Experimentally Validated and Parameterized Periodic Unit-cell Reconstruction of Open-cell Foams, *J. Appl. Phys.*, **109**, 2011, 130519-1–130519-10.
- [4] De Jaeger, P., T'Joel, C., Huisseune, H., Ameel, B., De Schampheleire, S. and De Paepe, M., Assessing the influence of four bonding methods on the thermal contact resistance of open-cell aluminum foam, *Int. J. Heat and Mass Transfer*, **55**, 2012, 6200–6210.
- [5] Fiedler, T., Belova, I.V. and Murch, G.E., Critical Analysis of the Experimental Determination of the Thermal Resistance of Metal Foams, *Int. J. Heat and Mass Transfer*, **55**, 2012, 4415–4420.
- [6] Ghosh, I., Heat Transfer Correlation for High-porosity Open-Cell Foam, *Int. J. Heat and Mass Transfer*, **52**, 2009, 1488–1494.
- [7] Hsieh, W.H., Wu, J.Y., Shih, W.H. and Chiu, W.C., Experimental Investigation of Heat-transfer Characteristics of Aluminum-foam Heat Sinks, *Int. J. Heat and Mass Transfer*, **47**, 2004, 5149–5157.
- [8] Incropera, F.P., DeWitt, D.P., Bergman, T.L. and Lavine, A.S., *Fundamentals of Heat and Mass Transfer - Sixth Edition*, Wiley, 2006.
- [9] Kim, S.Y., Paek, J.W. and Kang, B.H., Flow and Heat Transfer Correlations for Porous Fin in a Plate-Fin Heat Exchanger, *J. Heat Transfer - Trans. ASME*, **122**, 2000, 572–578.
- [10] Mahjoob, S. and Vafai, K., A Synthesis of Fluid and Thermal Transport Models for Metal Foam Heat Exchangers, *Int. J. Heat and Mass Transfer*, **51**, 2008, 3701–3711.
- [11] Tadrist, L., Miscovic, M., Rahli, O. and Topin, F., About the Use of Fibrous Materials in Compact Heat Exchangers, *J. Exper. Therm. Fluid Sci.*, **28**, 2004, 193–199.
- [12] Tamayol, A. and Hooman, K., Thermal Assessment of Forced Convection through Metal Foam Heat Exchangers, *J. Heat Transfer - Trans. of the ASME*, **133**, 2011, 1–7.
- [13] T'Joel, C., De Jaeger, P., Huisseune, H., Van Herzele, S., Vorst, N. and De Paepe, M., Thermo-hydraulic Study of a Single Row Heat Exchanger Consisting of Metal Foam Covered Round Tubes, *Int. J. Heat and Mass Transfer*, **53**, 2010, 3262–3274.